

# Controlling quantum transport through a single molecule

D. M. Cardamone, C. A. Stafford, S. Mazumdar

*Department of Physics, University of Arizona, 1118 E. 4th Street, Tucson, AZ 85721*

(Dated: October 30, 2018)

We investigate multi-terminal quantum transport through single monocyclic aromatic annulene molecules, and their derivatives, using the nonequilibrium Green function approach in the self-consistent Hartree-Fock approximation. A new device concept, the Quantum Interference Effect Transistor (QuIET) is proposed, exploiting perfect destructive interference stemming from molecular symmetry, and controlling current flow by introducing decoherence and/or elastic scattering that break the symmetry. This approach overcomes the fundamental problems of power dissipation and environmental sensitivity that beset many nanoscale device proposals.

PACS numbers: 85.65.+h, 73.63.-b, 31.15.Ne, 03.65.Yz

From the vacuum tube to the modern CMOS transistor, devices which control the flow of electrical current by modulating an electron energy barrier are ubiquitous in electronics. In this paradigm, a minimum energy of  $k_B T$  must be dissipated to switch the current “on” and “off,” necessitating incredible power dissipation at device densities approaching the atomic limit [1]. A possible alternative is to control electron flow using quantum interference [2, 3, 4, 5]. In mesoscopic devices, quantum interference is typically tuned via the Aharonov-Bohm effect [6]; however, in nanoscale conductors such as single molecules, this is impractical due to the enormous magnetic fields required to produce a phase shift of order one radian. Similarly, a device based on an electrostatic phase shift [3, 4] would, in small molecules, require voltages incompatible with structural stability. We propose a solution exploiting perfect destructive interference stemming from molecular symmetry, and controlling quantum transport by introducing decoherence or scattering from a third lead.

As daunting as the fundamental problem of the switching mechanism, is the practical problem of nanofabrication [1]. In this respect, single molecules have a distinct advantage over other types of nanostructures, in that large numbers of identical devices can be readily synthesized. Single-molecule devices with two leads have been fabricated by a number of techniques [7]. Our transistor requires a third terminal coupled locally to the molecule, capacitively or via tunneling (see Fig. 1). To date, only global gating of single-molecule devices has been achieved [7]; recently, however, there has been significant progress toward a locally coupled third terminal [8].

This Letter reports the results of our recent theoretical investigations into the use of interference effects to create molecular transistors, leading to a new device concept, which we call the Quantum Interference Effect Transistor (QuIET). We demonstrate that for all monocyclic aromatic annulenes, particular two-terminal configurations exist in which destructive interference blocks current flow, and that transistor behavior can be achieved by supplying tunable decoherence or scatter-

ing at a third site. We also propose a realistic model for introducing scattering in a controllable way, using an alkene chain of arbitrary length (*cf.* Fig. 1). Finally, we present nonequilibrium Green function (NEGF) calculations within the self-consistent Hartree-Fock approximation, indicating that the QuIET functions at room temperature with a current-voltage characteristic strikingly similar to macroscale transistors.

The Hamiltonian of the system can be written as the sum of three terms:  $H = H_{mol} + H_l + H_{tun}$ . The first is the  $\pi$ -electron molecular Hamiltonian

$$H_{mol} = \sum_{n\sigma} \epsilon_n d_{n\sigma}^\dagger d_{n\sigma} - \sum_{\langle nm \rangle \sigma} (t_{nm} d_{n\sigma}^\dagger d_{m\sigma} + \text{H.c.}) + \sum_{nm} \frac{U_{nm}}{2} Q_n Q_m, \quad (1)$$

where  $d_{n\sigma}^\dagger$  creates an electron of spin  $\sigma$  in the  $\pi$ -orbital of the  $n$ th carbon atom,  $\epsilon_n$  are the orbital energies, and  $\langle \rangle$  indicates a sum over nearest neighbors. The tight-

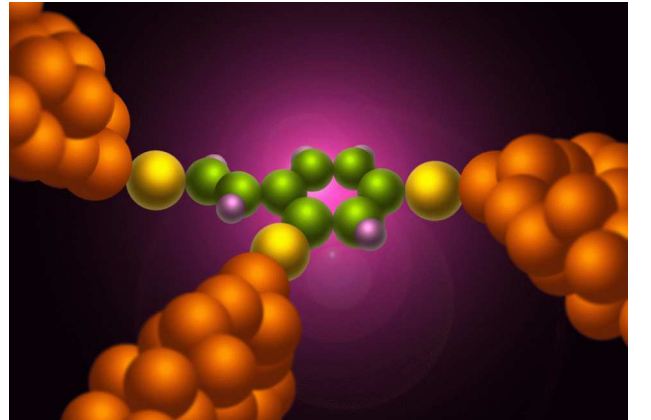


FIG. 1: Artist’s conception of a Quantum Interference Effect Transistor (QuIET). The colored spheres represent individual carbon (green), hydrogen (purple), and sulfur (yellow) atoms, while the three gold structures represent the metallic contacts. A voltage applied to the leftmost contact regulates the flow of current between the other two.

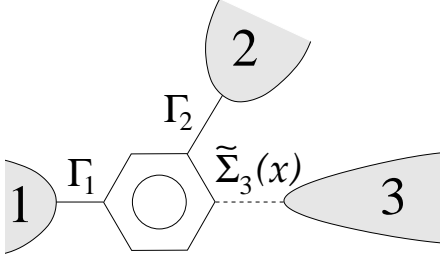


FIG. 2: Schematic diagram of a QuIET based on benzene. Here  $\Gamma_{1,2}$  are the coupling strengths of metallic leads 1 and 2, connected in the meta orientation, to the corresponding  $\pi$ -orbitals of benzene.  $\tilde{\Sigma}_3$ , determined by a control variable  $x$ , is the retarded self-energy induced by lead 3. The real part of  $\tilde{\Sigma}_3$  introduces elastic scattering, while the imaginary part introduces decoherence.

binding hopping matrix elements  $t_{nm} = 2.2\text{eV}$ ,  $2.6\text{eV}$ , or  $2.4\text{eV}$  for orbitals connected by a single bond, double bond, or within an aromatic ring, respectively. The final term of Eq. (1) contains intra- and intersite Coulomb interactions, as well as the electrostatic effects of the leads. The interaction energies are given by the Ohno parameterization [9, 10]:

$$U_{nm} = \frac{11.13\text{eV}}{\sqrt{1 + .6117 (R_{nm}/\text{\AA})^2}}, \quad (2)$$

where  $R_{nm}$  is the distance between orbitals  $n$  and  $m$ .  $Q_n = \sum_{\sigma} d_{n\sigma}^{\dagger} d_{n\sigma} - \sum_{\alpha} C_{n\alpha} \mathcal{V}_{\alpha} / e - 1$  is an effective charge operator [11] for orbital  $n$ , where the second term represents a polarization charge. Here  $C_{n\alpha}$  is the capacitance between orbital  $n$  and lead  $\alpha$ , chosen consistent with the interaction energies of Eq. (2) and the geometry of the device, and  $\mathcal{V}_{\alpha}$  is the voltage on lead  $\alpha$ .  $e$  is the magnitude of the electron charge.

Each metal lead  $\alpha$  possesses a continuum of states, and their total Hamiltonian is

$$H_l = \sum_{\alpha} \sum_{\substack{k \in \alpha \\ \sigma}} \epsilon_k c_{k\sigma}^{\dagger} c_{k\sigma}, \quad (3)$$

where  $\epsilon_k$  are the energies of the single-particle levels in the leads, and  $c_{k\sigma}^{\dagger}$  is an electron creation operator. Tunneling between molecule and leads is provided by the final term of the Hamiltonian,

$$H_{tun} = \sum_{\langle n\alpha \rangle} \sum_{\substack{k \in \alpha \\ \sigma}} (V_{nk} d_{n\sigma}^{\dagger} c_{k\sigma} + \text{H.c.}), \quad (4)$$

where  $V_{nk}$  are the tunneling matrix elements from a level  $k$  within lead  $\alpha$  to the nearby site  $n$ . Coupling of the leads to the molecule via molecular chains, as may be desirable for fabrication purposes, can be included in the effective  $V_{nk}$ , as can the effect of substituents (e.g., thiol groups) used to bond the leads to the molecule [12, 13].

We use the NEGF approach [14, 15] to describe transport in this open quantum system. Given the retarded Green function of the isolated molecular system  $G_{mol}(E) = (E - H_{mol} + i0^+)^{-1}$ , Dyson's equation

$$G(E) = [G_{mol}^{-1}(E) - \Sigma(E)]^{-1} \quad (5)$$

gives the Green function of the full system. The QuIET is intended for use at room temperature and above, and operates in a voltage regime where there are no unpaired electrons in the molecule. Thus lead-lead and lead-molecule correlations, such as the Kondo effect, do not play an important role. Electron-electron interactions may therefore be included via the self-consistent Hartree-Fock method [16].  $H_{mol}$  is replaced by the corresponding mean-field Hamiltonian  $H_{mol}^{HF}$ , which is quadratic in electron creation and annihilation operators, and contains long-range hopping. Within mean-field theory, the retarded self-energy due to the leads is

$$\Sigma_{n\sigma, m\sigma'}(E) = -\frac{i}{2} \delta_{nm} \delta_{\sigma\sigma'} \sum_{\langle a\alpha \rangle} \Gamma_{\alpha}(E) \delta_{na}, \quad (6)$$

where  $\Gamma_{\alpha}(E) = 2\pi \sum_{k \in \alpha} |V_{nk}|^2 \delta(E - \epsilon_k)$  is the Fermi's Golden Rule tunneling width. As a result, the molecular density of states changes from a discrete spectrum of delta functions to a continuous, width-broadened distribution. We take the broad-band limit [14], treating  $\Gamma_{\alpha}$  as constants characterizing the coupling of the leads to the molecule. Typical estimates [13] using the method of Ref. [17] yield  $\Gamma_{\alpha} \lesssim 0.5\text{eV}$ , but values as large as  $1\text{eV}$  have been suggested [12].

The effective hopping and orbital energies in  $H_{mol}^{HF}$  depend on the equal-time correlation functions, which are found in the NEGF approach to be

$$\langle d_{n\sigma}^{\dagger} d_{m\sigma} \rangle = \sum_{\langle a\alpha \rangle} \frac{\Gamma_{\alpha}}{2\pi} \int_{-\infty}^{\infty} dE G_{n\sigma, a\sigma}(E) G_{a\sigma, m\sigma}^*(E) f_{\alpha}(E), \quad (7)$$

where  $f_{\alpha}(E) = \{1 + \exp[(E - \mu_{\alpha})/k_B T]\}^{-1}$  is the Fermi function for lead  $\alpha$ . Finally, the Green function is determined by iterating the self-consistent loop, Eqs. (5)–(7).

The current in lead  $\alpha$  is given by the multi-terminal current formula [18]

$$I_{\alpha} = \frac{2e}{h} \sum_{\beta} \int_{-\infty}^{\infty} dE T_{\beta\alpha}(E) [f_{\beta}(E) - f_{\alpha}(E)], \quad (8)$$

where  $T_{\beta\alpha}(E) = \Gamma_{\beta} \Gamma_{\alpha} |G_{ba}(E)|^2$  is the transmission probability [15] from lead  $\alpha$  to lead  $\beta$ , and  $a$  ( $b$ ) is the orbital coupled to lead  $\alpha$  ( $\beta$ ).

The QuIET exploits quantum interference stemming from the symmetry of monocyclic aromatic annulenes, such as benzene. Quantum transport through single benzene molecules with two metallic leads connected in the *para* orientation has been the subject of extensive experimental and theoretical investigation [7]; however, a

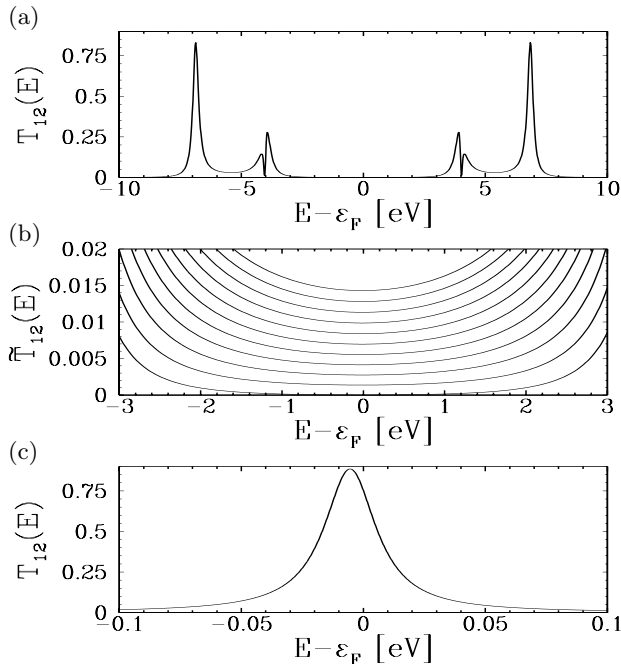


FIG. 3: Effective transmission probability  $\tilde{T}_{12}$  of the device shown in Fig. 2, at room temperature, with  $\Gamma_1 = 1.2\text{eV}$  and  $\Gamma_2 = .48\text{eV}$ : (a)  $\tilde{\Sigma}_3 = 0$ ; (b)  $\tilde{\Sigma}_3 = -i\Gamma_3/2$ , where  $\Gamma_3 = 0$  in the lowest curve and increases by .24eV in each successive one; (c)  $\tilde{\Sigma}_3$  is given by Eq. (10) with a single resonance,  $\varepsilon_\nu = \varepsilon_F$  and  $t_\nu = 1\text{eV}$ .

QuiET based on benzene requires the source (1) and drain (2) to be connected in a *meta* orientation, as illustrated in Fig. 2. An electron propagating between leads 1 and 2 takes all possible paths within the molecule. In the absence of a third lead ( $\tilde{\Sigma}_3 = 0$ ), these paths all lie within the benzene ring. In linear response, and with no net charge transfer between molecule and leads, each electron injected into the molecule has momentum given by its Fermi wavenumber,  $k_F = \pi/2d$ , where  $d = 1.397\text{\AA}$  is the intersite spacing of benzene. The phase difference between the two most direct paths through the ring is  $\pi$ , and they interfere destructively. Similarly, all of the paths through the ring cancel exactly in a pairwise fashion. It is a consequence of Luttinger's Theorem [19] that this coherent suppression of current is not altered by electron-electron interactions.

Figure 3a shows the transmission probability  $T_{12}$  of the device shown in Fig. 2 for  $\tilde{\Sigma}_3(E) = 0$ , illustrating the total current suppression at the Fermi energy (see also Fig. 3b, lowest curve). This suppression can be lifted by introducing decoherence or elastic scattering that break the molecular symmetry. Figures 3b and c illustrate the effect of attaching a third lead to the molecule as shown in Fig. 2, introducing a complex self-energy  $\tilde{\Sigma}_3(E)$  on the  $\pi$ -orbital adjacent to that connected to lead 2.

An imaginary self-energy  $\tilde{\Sigma}_3 = -i\Gamma_3/2$  corresponds to coupling a third metallic lead directly to the ben-

zene molecule. If the third lead functions as an infinite-impedance voltage probe, the effective two-terminal transmission is [20]

$$\tilde{T}_{12} = T_{12} + \frac{T_{13}T_{32}}{T_{13} + T_{32}}. \quad (9)$$

The third lead introduces decoherence [20] and additional paths that are not cancelled, thus allowing current to flow, as shown in Fig. 3b. As a proof of principle, a QuiET could be constructed using a scanning tunneling microscope tip as the third lead, with tunneling coupling  $\Gamma_3(x)$  to the appropriate  $\pi$ -orbital of the benzene ring, the control variable  $x$  being the piezo-voltage controlling the tip-molecule distance.

By contrast, a real self-energy  $\tilde{\Sigma}_3$  introduces elastic scattering, which can also break the molecular symmetry. This can be achieved by attaching a second molecule to the benzene ring, for example an alkene chain (*cf.* Fig. 1). The retarded self-energy due to the presence of a second molecule is

$$\tilde{\Sigma}_3(E) = \sum_\nu \frac{|t_\nu|^2}{E - \varepsilon_\nu + i0^+}, \quad (10)$$

where  $\varepsilon_\nu$  is the energy of the  $\nu$ th molecular orbital of the second molecule, and  $t_\nu$  is the hopping integral coupling this orbital with the indicated site of benzene. The side-group introduces Fano antiresonances [21], which block current through one arm of the annulene, thus lifting the destructive interference. Put another way, the second molecule's orbitals hybridize with those of the annulene, and a state that connects leads 1 and 2 is created in the gap (see Fig. 3c). Shifting  $\varepsilon_\nu$  by gating the sidegroup then yields transistor action.

Tunable current suppression occurs over a broad energy range, as shown in Fig. 3b; the QuiET functions with any metallic leads whose work function lies within the annulene gap. Fortunately, this is the case for many bulk metals, among them palladium, iridium, platinum, and gold [16]. Appropriately doped semiconductor electrodes [8] could also be used.

In Fig. 4, the  $I$ - $V$  characteristic of a QuiET based on sulfonated vinyl benzene is shown, whose molecular structure is given in Fig. 1. The three metallic electrodes were taken as bulk gold, with  $\Gamma_1 = \Gamma_2 = 1\text{eV}$ , while  $\Gamma_3 = .0024\text{eV}$ , so that the coupling of the third electrode to the alkene sidegroup is primarily electrostatic. The device characteristic resembles that of a macroscopic transistor. As the voltage on lead 3 is increased, the antibonding orbital of the alkene sidegroup comes into resonance with the Fermi energies of leads 1 and 2, leading to a broad peak in the current. For  $\Gamma_{1,2} \gg \Gamma_3 \neq 0$ , the device amplifies the current in the third lead (dotted curve), emulating a bipolar junction transistor. For  $\Gamma_3 = 0$ , the calculated current  $I_1$  is almost identical to that shown in Fig. 4, and the device acts like a field effect transistor.

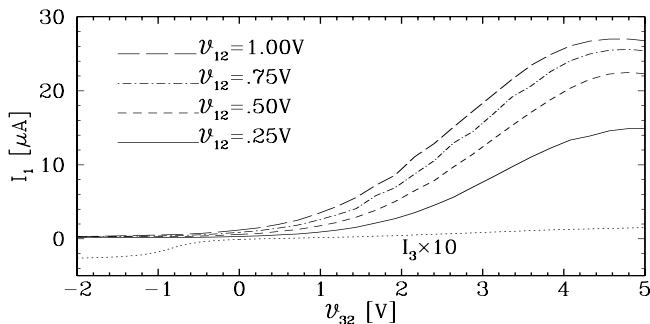


FIG. 4:  $I$ - $V$  characteristic of the QuIET shown in Fig. 1 at room temperature. The current in lead 1 is shown, where  $V_{\alpha\beta} = V_{\alpha} - V_{\beta}$ . Here,  $\Gamma_1 = \Gamma_2 = 1\text{eV}$ .  $\Gamma_3$  is taken as  $.0024\text{eV}$ , which allows a small current in the third lead, so that the device amplifies current. A field-effect device with almost identical  $I$ - $V$  can be achieved by taking  $\Gamma_3 = 0$ . The curve for  $I_3$  is for the case of  $1.00\text{V}$  bias voltage;  $I_3$  for other biases look similar.

Alkene chains containing 4 and 6 carbon atoms were also studied, yielding devices with characteristics similar to that shown in Fig. 4, with the maximum current  $I_1$  shifting to smaller values of  $V_{32}$  with increasing chain length. As evidence that the transistor behavior shown in Fig. 4 is due to the tunable interference mechanism discussed above, we point out that if hopping between the benzene ring and the alkene sidegroup is set to zero, so that the coupling of the sidegroup to benzene is purely electrostatic, almost no current flows between leads 1 and 2.

Operation of the QuIET does not depend sensitively on the magnitude of the lead-molecule coupling  $\bar{\Gamma} = \Gamma_1\Gamma_2/(\Gamma_1 + \Gamma_2)$ . The current through the device decreases with decreasing  $\bar{\Gamma}$ , but aside from that, the device characteristic was found to be qualitatively similar when  $\bar{\Gamma}$  was varied over one order of magnitude.

The QuIET mechanism applies to any monocyclic aromatic annulene with leads 1 and 2 positioned so the two most direct paths have a phase difference of  $\pi$ . Furthermore, larger molecules have other possible lead configurations, based on phase differences of  $3\pi$ ,  $5\pi$ , etc. Figure 5 shows the lead configurations for a QuIET based on [18]-annulene.

The position of the third lead affects the degree to which destructive interference is suppressed. For benzene, the most effective location for the third lead is shown in Figs. 1 and 2. It may also be placed at the site immediately between leads 1 and 2, but the transistor effect is somewhat reduced, since coupling to the charge carriers is less. The third, three-fold symmetric configuration of leads completely decouples the third lead from electrons travelling between the first two leads. For each monocyclic aromatic annulene, one three-fold symmetric lead configuration exists, yielding no transistor behavior.

The QuIET's operating mechanism, tunably coherent current suppression, occurs over a broad energy range

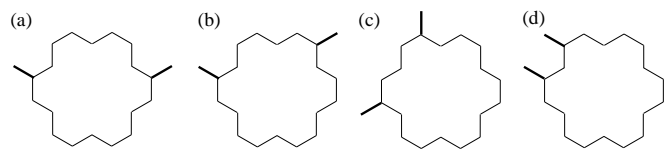


FIG. 5: Source-drain lead configurations possible in a QuIET based on [18]-annulene. The bold lines represent the positioning of the two leads. Each of the four arrangements has a different phase difference associated with it: (a)  $\pi$ ; (b)  $3\pi$ ; (c)  $5\pi$ ; and (d)  $7\pi$ .

within the gap of each monocyclic aromatic annulene; it is thus a *very robust effect, insensitive to moderate fluctuations of the electrical environment of the molecule*. Although based on an entirely different, quantum mechanical, switching mechanism, the QuIET nonetheless reproduces the functionality of macroscopic transistors on the scale of a single molecule.

This work was supported by National Science Foundation Grant Nos. PHY0210750, DMR0312028, and DMR0406604, and PHY0244389.

- 
- [1] *International technology roadmap for semiconductors: 2004 update*, <http://public.itrs.net>.
  - [2] P. Sautet and C. Joachim, Chem. Phys. Lett. **153**, 511 (1988).
  - [3] F. Sols, M. Macucci, U. Ravaioli, and K. Hess, Appl. Phys. Lett. **54**, 350 (1989).
  - [4] R. Baer and D. Neuhauser, J. Am. Chem. Soc. **124**, 4200 (2002).
  - [5] R. Stadler, M. Forshaw, and C. Joachim, Nanotechnology **14**, 138 (2003).
  - [6] S. Washburn and R. A. Webb, Adv. Phys. **35**, 375 (1986).
  - [7] A. Nitzan and M. A. Ratner, Science **300**, 1384 (2003), and references therein.
  - [8] P. G. Piva *et al.*, Nature **435**, 658 (2005).
  - [9] K. Ohno, Theor. Chim. Acta **2**, 219 (1964).
  - [10] M. Chandross, S. Mazumdar, M. Liess, P. A. Lane, Z. V. Vardeny, M. Hamaguchi, and K. Yoshino, Phys. Rev. B **55**, 1486 (1997).
  - [11] C. A. Stafford, R. Kotlyar, and S. Das Sarma, Phys. Rev. B **58**, 7091 (1998).
  - [12] W. Tian *et al.*, J. Chem. Phys. **109**, 2874 (1998).
  - [13] A. Nitzan, Annu. Rev. Phys. Chem. **52**, 681 (2001).
  - [14] A.-P. Jauho, N. S. Wingreen, and Y. Meir, Phys. Rev. B **50**, 5528 (1994).
  - [15] S. Datta, *Electronic Transport in Mesoscopic Systems* (Cambridge University Press, Cambridge, UK, 1995).
  - [16] M. P. Marder, *Condensed Matter Physics* (John Wiley & Sons, Inc., New York, 2000).
  - [17] V. Mujica, M. Kemp, and M. A. Ratner, J. Chem. Phys. **101**, 6849 (1994).
  - [18] M. Büttiker, Phys. Rev. Lett. **57**, 1761 (1986).
  - [19] J. M. Luttinger, Phys. Rev. **119**, 1153 (1960).
  - [20] M. Büttiker, IBM J. Res. Dev. **32**, 63 (1988).
  - [21] A. A. Clerk, X. Waintal, and P. W. Brouwer, Phys. Rev. Lett. **86**, 4636 (2001).